Chiral self-organized single 2D-layers of tetramers from a functional donor-acceptor molecule by the surface template effect

Anna J. Kny,[†] Max Reimer,[‡] Noah Al-Shamery,[†] Ritu Tomar,[†] Thomas Bredow,[†]
Selina Olthof,[‡] Dirk Hertel,[‡] Klaus Meerholz,[‡] and Moritz Sokolowski[*,†]

[†]*Clausius-Institut für Physikalische und Theoretische Chemie, Universität Bonn, Wegelerstraße 12, 53115 Bonn, Germany*
[‡]*Department Chemie, Universität zu Köln, Greinstraße 4-6, 50939 Köln, Germany*

E-mail: sokolowski@pc.uni-bonn.de

Additional Information on Experimental Details and DFT Calculations

Sample Preparation and Low Energy Electron Diffraction (LEED)

All experiments were carried out under ultra high vacuum (UHV) conditions at a base pressure of 3×10^{-10} mbar. The Ag(100) surface was prepared by sputtering with Ar ions for 20 min (1×10^{-5} mbar Ar, 1 keV, 5 µA, 300 K) and subsequent annealing at 600 K for ∼30 min. The surface quality was controlled by LEED. A multi-channel plate (MCP) LEED manufactured by OCI Vacuum Microengineering was used for verifying the structural order of the samples for the XPS/UPS and STM measurements. A SPA-LEED manufactured by Omicron NanoTechnology was used for detailed structural analysis. The sample preparation was optimized to yield large terraces. As a consequence of prolonged annealing, the monoatomic Ag steps are partly pinned at segregated surface impurities. This causes that long step edges exhibit a curved shape as it can be seen in Figure 2(a).

The **HB238** was synthesized and purified following the route of Bürckstümmer et al.[1] Photos of a three dimensional model are shown in Figure S1 in order to illustrate its steric structure. A homebuilt Knudsen cell was used for the deposition of the **HB238** using a crucible temperature of 310 °C. During the deposition, the Ag(100) sample was kept at room temperature. Notably, at low sample temperatures of about 110 K, no ordered structures were obtained due to kinetic reasons. The deposition was controlled by a quadrupole mass spectrometer, 200 Prisma of the company Balzer/Pfeiffer. Because the molecular mass of **HB238** (426.19 g/mol) exceeds the range of this mass spectrometer, we monitored $m/z = 57$ amu/e. Given coverages refer to the coverage of one monolayer (1 ML) which resembles a closed layer of face-on adsorbed molecules in the α-phase. Typical deposition rates were about 0.4 ML/min.

The SPA-LEED instrument was operated at beam currents of about 1 nA. In order to minimize the thermal background, the sample was cooled by liquid nitrogen to 110 K. The brightness and the contrast of the image shown

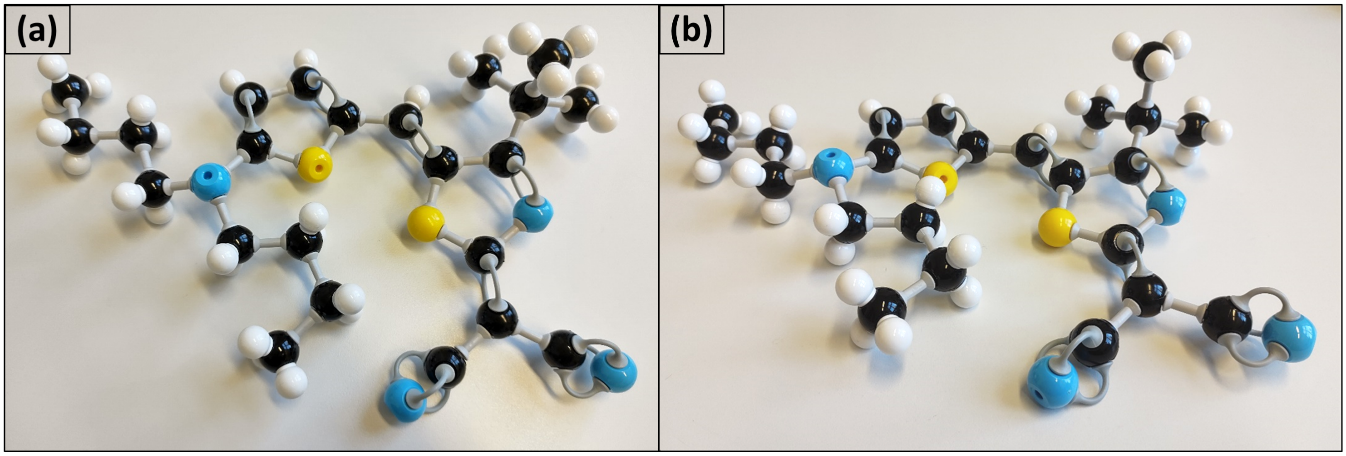

Figure S1: Three dimensional model of **HB238** (R enantiomer). The upward pointing *tert*-butyl group which is responsible for the prominent lobes observed in the STM images of the α-phase, is located in the upper right corner of each image. (a) Top view. (b) Inclined view. Color code: white: H, black: C, blue: N, and yellow: S atoms.

in Figure 2(d) were adjusted, and an additional background subtraction was performed. Prior to evaluation, the LEED patterns were deskewed using a software package developed by F. Sojka.[2] The parameters for the deskewing were obtained from recording a SPA-LEED pattern of the commensurate monolayer of PTCDA on Ag(100).[3] The kinematic simulations of the measured patterns were performed with the programs Spot-Plotter[4] and LEEDLab.[2,5]

Scanning Tunneling Microscopy

STM-measurements were done with an UHV 300 STM built by the company RHK Technology and self-cut Pt/Ir-tips (90:10) in constant current mode. Given bias voltages U_{bias} refer to the sample. The sample was cooled by a reduced flow of liquid He to obtain sample temperatures between 34 and 300 K. We had to use very low tunneling currents I_{t} of the order of 5 to 10 pA to obtain stable imaging conditions. At higher currents the molecules were easily displaced by tip sample interactions that are enhanced at smaller tip sample distances required for larger tunneling currents. Routinely, we measured at negative bias voltages. Measurements performed at positive bias voltages were less stable, but provided comparable structural information. For corrections and evaluation of the STM data the software Gwyddion[6] was used. For better visibility of the molecular structures, the brightness and contrast of the STM images were corrected. Error lines, caused by noise, were removed by the fractal correction of the Gwyddion program.[6] The STM images were deskewed such that the lattice fitted to the SPA-LEED data. This procedure corrects the distortions caused by the creep (drift caused by the piezoelectric elements) and thermal drift. STM images of the α-phase at high magnification were finally processed by the correlation averaging tool of the software WSxM.[7]

Photoemission Spectroscopy

UPS measurements were conducted with a helium discharge lamp (He-I, 21.22 eV, at a bias voltage of −8 V) at a pass energy of 2 eV, with an energy resolution (as determined by the width of the Fermi edge) of 110 meV, using a Phoibos 100 hemispherical analyzer (manufactured by Specs) under normal emission. The electron binding energy scale was calibrated using the Fermi edge of a cleaned gold substrate. X-ray photoemission spectroscopy (XPS) measurements were performed with synchrotron light at the beamline I09 at the Diamond Light Source. A hemispherical analyzer was used and electrons were collected within an emission cone of 56° and an average angle of 45° with respect to the surface normal in the plane of the polarization of the synchrotron light. Photon energies (E_γ) were chosen such that the kinetic energies of the photoelectrons were about 100 eV. Indications for dissociation of molecules upon adsorption were only marginal, i.e., a small peak of about 6% of the total intensity of the S$2p_{3/2}$ peak is observed at 161.75 eV for the monolayer (outside the displayed range of Figure 3). It is presumably related to a small fraction of dissociated molecules at surface defects.[8]

DFT Calculations

The minimum energy structure for an isolated **HB238** molecule was obtained by performing density functional theory (DFT) calculations on 356 conformers which were obtained by using the conformer-rotamer ensemble sampling tool (CREST).[9] DFT calculations were performed with the program ORCA 4.2.1[10] using the Perdew-Burke-Ernzerhof (PBE)[11] functional and the def2-TZVPP basis sets.[12]

Additional information concerning the structure of the β-phase

The information content of STM data of the β-phase is more limited, compared to the α-phase, likely due to the edge-on orientation of the molecules in this phase and makes structural conclusions more speculative. However, here we amend some aspects that can be derived from the spatial demand of the molecules already.

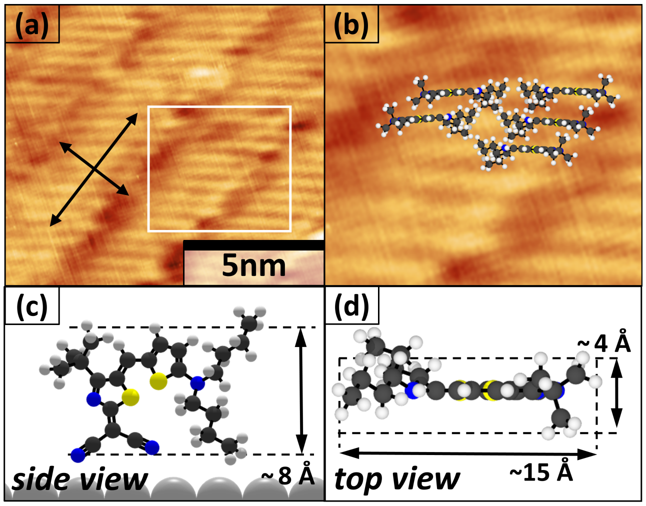

Figure S2: Small scale STM image of the β-phase and hardsphere model. (**a**) STM image of the β-phase (T=40 K, U_{bias}=−0.29 V; I_{t}=5.4 pA). The black arrows indicate the long and short axes of the aggregate. (**b**) Zoom-in of the region marked by the white frame in (a) superimposed by a proposed model showing five molecules. (**c, d**) Side- and top-view of a hardsphere model of **HB238** showing the molecule in edge-on orientation with respect to the Ag surface with indicated geometric dimensions (van der Waals radii reduced by a factor of 0.3). Structural details of the molecule, in particular of the flexible side groups, and the adsorption site on the Ag(100) surface are experimentally unconfirmed (white: H, dark gray: C, blue: N, and yellow: S atoms).

Figures S2(a) and (b) display an STM image of the β-phase and a respective zoom-in, which is overlain by a model comprising five molecules. Notable is the striped fine structure of the aggregates (in vertical direction of Figs. S2(a)/(b)) with a periodicity of 4.7±1 Å, which was already mentioned in the main text. From comparison with the steric demand of a molecule in an edge-on orientation with respect to the surface, we conclude that this fine structure is related to a coplanar π-stacking of the molecules. The geometric dimensions of one molecule in this orientation are indicated in the side- and top-views of the hardsphere model in Figures S2(c) and (d). The estimated thickness of the molecule in the direction perpendicular to the π-system of $\sim$ 4 Å fits to the measured spacing of 4.7±1 Å. The molecule is oriented with its CN-groups to the surface, which is plausible from a chemical point of view.

In the direction of the stripes (horizontal direction in Fig. S2(a)) the aggregates exhibit a width of ∼15 or ∼30 Å which corresponds to the length of one or two molecules in edge-on orientation. An example for the former case is given by the aggregates shown in Figure 2(c) in the main text, whereas an example for the latter is shown in Figure S2(b) (above). Hence, we propose that the aggregates are stacks of monomers or dimers. A clear topographic separation of the two molecules forming a dimer, which is expected at about the middle of the aggregate, is not seen (s. Fig. S2(b)). On the other hand, the aggregates can be clearly distinguished from each other. A possible explanation could be that the dimer formation is caused by the intertwining of opposing *n*-butyl groups from two molecules in tail-to-tail arrangement, leading to a constant apparent height in the STM image. Differently, the *tert*-butyl groups pointing to the edges of the aggregate cause a topographic separation from the neighboring aggregates that is imaged. This is illustrated in the tentative model in Figure S2(b).

The electrostatic interactions between neighboring molecules and the sterical demand of the *tert*-butyl-groups are the likely reasons that disfavor a simple coin-role-like stacking of the **HB238** molecules. Thus, lateral shifts between the molecules in the direction of the molecular axis and parallel to the surface occur. These varying shifts between the molecules cause changes in the direction of the long axis of the aggregates, which also lead to an inclination of the molecules with respect to the short axis of the aggregate (e.g., by 40° to 50° in Fig. S2(a)/(b)). As a result, the length of the short axis of the aggregate (perpendicular to the long one) can vary, which promotes a dense packing of the aggregates into larger domains (for examples cf. Fig. 2(c) in the main text).

References

(1) Bürckstümmer, H.; Tulyakova, E. V.; Deppisch, M.; Lenze, M. R.; Kronenberg, N. M.; Gsänger, M.; Stolte, M.; Meerholz, K.; Würthner, F. Efficient Solution-Processed Bulk Heterojunction Solar Cells by Antiparallel Supramolecular Arrangement of Dipolar Donor–Acceptor Dyes. *Angew. Chem. Int. Ed.* **2011**, *50*, 11628–11632.

(2) Sojka, F.; Meissner, M.; Zwick, C.; Forker, R.; Fritz, T. Determination and correction of distortions and systematic errors in low-energy electron diffraction. *Rev. Sci. Instrum.* **2013**, *84*, 015111.

(3) Ikonomov, J.; Bauer, O.; Sokolowski, M. Highly ordered thin films of perylene-3,4,9,10-tetracarboxylic acid dianhydride (PTCDA) on Ag(100). *Surf. Sci.* **2008**, *602*, 2061–2068.

(4) Bayersdorfer, P. "Spot-Plotter Version 1.2.1.4", Universität Würzburg. 2008.

(5) Sojka, F.; Fritz, T. "LEEDLab 2018 Version v1.2", Fritz & Sojka GbR, Apolda. 2019.

(6) Necas, D.; Klapetek, P. Gwyddion: an open-source software for SPM data analysis. *Cent. Eur. J. Phys.* **2012**, *10*, 181–188.

(7) Horcas, I.; Fernández, R.; Gómez-Rodríguez, J. M.; Colchero, J.; Gómez-Herrero, J.; Baro, A. M. WSXM: A software for scanning probe microscopy and a tool for nanotechnology. *Rev. Sci. Instrum.* **2007**, *78*, 013705.

(8) Moulder, J. F.; Stickle, W. F.; Sobol, P. E.; Bomben, K. D. In *Handbook of X-ray Photoelectron Spectroscopy*; Chastain, J., Ed.; Perkin-Elmer Corporation, 1992.

(9) Pracht, P.; Bohle, F.; Grimme, S. Automated exploration of the low-energy chemical space with fast quantum chemical methods. *Phys. Chem. Chem. Phys.* **2020**, *22*, 7169–7192.

(10) Neese, F.; Wennmohs, F.; Becker, U.; Riplinger, C. The ORCA quantum chemistry program package. *J. Chem. Phys.* **2020**, *152*, 224108.

(11) Perdew, J. P.; Burke, K.; Ernzerhof, M. Generalized Gradient Approximation Made Simple. *Phys. Rev. Lett.* **1996**, *77*, 3865–3868.

(12) Weigend, F.; Ahlrichs, R. Balanced basis sets of split valence, triple zeta valence and quadruple zeta valence quality for H to Rn: Design and assessment of accuracy. *Phys. Chem. Chem. Phys.* **2005**, *7*, 3297–3305.